The Eurasia Proceedings of Science, Technology,
Engineering and Mathematics (EPSTEM)
ISSN: 2602-3199

The Eurasia Proceedings of Science, Technology, Engineering and Mathematics (EPSTEM), 2026

Volume 40, Pages 374-390

ICBAST 2026: International Conference on Basic Sciences and Technology

Power Supply Technologies for Collaborative Service Robots: Characteristics and Comparative Overview

Nina Valchkova
Bulgarian Academy of Sciences

Roman Zahariev
Bulgarian Academy of Sciences

Vasil Tsvetkov
Bulgarian Academy of Sciences

Yasen Paunski
Bulgarian Academy of Sciences

Georgi Angelov
Bulgarian Academy of Sciences

Abstract: The article examines the power supply of a Service Collaborative Robot, powered by a hydrogen fuel cell, intended for transporting seriously injured people and serving them in medical facilities. The qualities of this power supply are analyzed, highlighting its advantages in terms of environmental characteristics and its long "life" during the activities of serving patients in serious health conditions and transporting them to a hospital. Some main characteristics of this type of robot, powered by a hydrogen fuel cell, are analyzed, compared with robots powered by other types of power supplies, and its advantages when working in a hospital are shown.

Keywords: Service robot, Cobot, Hydrogen-powered robot.

Introduction

Power supply is a key element in the architecture of any mobile or stationary Collaborative Service Robot (Cobot) (CSR) (Kelly et al., 2021; Lynch et al., 2017). The duration of autonomous operation, functional capabilities and operational safety when interacting with people depend on its reliability, energy efficiency and safety (Miranda et al., 2025). An analysis of the state of the healthcare system justifies the increasing trend of creating robotic systems to assist medical personnel, especially after the development of the Covid 19 pandemic in recent years. When designing such a "cobot", a number of questions arise and it is important to answer them adequately. Creating such highly intelligent and "smart" robots is a difficult and extremely responsible task. In addition to the use of various sensors to provide information from the environment, on the basis of which a safe trajectory of movement of the robot itself and its manipulator is generated, management in the service process is carried out by recognizing voice commands, which is very important from the point of view of user convenience. The power supply system is of utmost importance for the long-lasting and trouble-free operation of the collaborative robot (Pa et al., 2016; Thounthong et al., 2009). The special requirements of these robots, designed to assist people with injuries or those in disadvantaged situations, in terms of the power supply system imply stable, uninterrupted and sufficiently long-term operation to fulfil the set goals. That is why it is necessary to develop and create power supply systems that, on the one hand, should be sufficiently compact and relatively light in weight, while at the

- Selection and peer-review under responsibility of the Organizing Committee of the Conference

same time having the ability and being able to release enough energy necessary to perform the complex tasks set by the supervisor.

- In this sense of reasoning, it is particularly important to make a comparison of the characteristics of the existing power supply systems for the collaborative robot and especially to highlight the advantages of the hydrogen fuel cell power supply, which is gaining increasing popularity.
- The energy that hydrogen provides is sufficient and is an alternative to fossil fuels with the potential to achieve the goals for the development of society *(Angelov, 2025)*. Hydrogen is found in many chemical compounds, such as water and organic biomass, and when burned, it releases heat energy – without pollutants or carbon dioxide. Increased energy consumption is a universal driver for improving the quality of life in all societies, from developing to developed countries. By supplying and using energy that improves the quality of life without endangering the environment, climate or geopolitical relations, the development effect is achieved. Hydrogen fuel cell technology is the subject of continuous research and development (Hasan et al., 2026). Hydrogen fuel cells are used as a clean and efficient alternative to traditional internal combustion engines, especially in the transport sector this sense of reasoning, it is particularly important to make a comparison of the characteristics of the existing power supply systems for the collaborative robot and especially to highlight the advantages of hydrogen fuel cell power supply, which is gaining increasing popularity (Ehsani et al, 2018).

Mobility Platform Analysis for Collaborative Mobile Robots

The mobility selection framework integrates quantitative and qualitative criteria using a multi-criteria decision-making (MCDM) approach. Key metrics include traction coefficient, ground pressure, energy consumption, obstacle negotiation capability, turning radius, and stability margin (Siciliano & Khatib, 2016). Advanced evaluation combines Analytical Hierarchy Process (AHP) for weighting and TOPSIS for ranking alternatives across diverse terrains and mission profiles.

Experimental Validation Framework

Experimental validation includes real-world tests and simulation-based evaluation. Metrics include traction force measurements, rollover stability, climbing angle, energy profiles under various terrains, and mobility autonomy. These tests validate theoretical models and guide optimization of hybrid systems.

Mathematical Models of Mobility Systems

Mathematical modeling includes kinematic equations, dynamic models, and energy consumption formulations. Differential drive equations, track-ground interaction models, and legged mobility gait models form the analytical basis (Li et al., 2019; McGrew et al., 2020).

Comparative Table of Mobile Platform Mobility Types

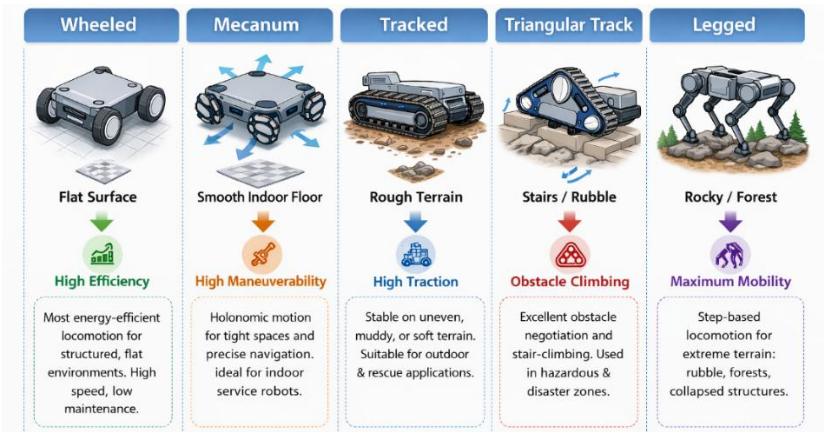

Figure 1 . Decision-flow for selecting energy supply architectures in collaborative service robots

The selection of an appropriate mobility platform is a critical design decision in collaborative mobile robotic systems. The methodology for mobility selection involves evaluating operational requirements, environmental constraints, mechanical complexity, and energy efficiency. The analysis presented in Figure 1 demonstrates that no single mobility type is universally optimal; instead, each provides distinct trade-offs.

Balance in the Choice of Power Supply for the Collaborative Robot

In collaborative robotics, a balance is sought in the power supply between high energy density, low weight, safety and the possibility of quick recharging or replacement (Chinta et al., 2025). The following table, Table 1 provides the characteristics of the types of power supply for the collaborative robot, so that a comparison can be made between each of them.

Criteria for Selecting the Type of Power Supply

Of course, there is a system of criteria for selecting the power supply for a collaborative robot intended for work in a medical facility. These requirements are determined by the specifics of the robot's activity and are relatively strict enough to obtain the expected effect of its activity (Delgado et al., 2025). For example, several such criteria can be listed as follows:

Table 1. Comparison of power supply technologies for collaborative service robots

Power supply type	Characteristics	Advantages	Disadvantages	Typical applications
1. Battery (electrochemical)	Lithium-ion, lithium-polymer, lithium-iron phosphate, nickel-metal hydride cells.	High energy density, compactness, suitable for mobility.	Limited life (cycles), risk of overheating, need for BMS.	Most mobile CSR - hospital assistants, logistics and disinfection robots.
2. Hybrid power supply. (battery + supercapacitors)	Combination of fast-discharge and long-life sources.	Extended battery life, ability to absorb peak loads. .	More complex control electronics.	Robots with high starting currents (manipulators, AGV).
3. Fuel cell power supply (hydrogen or methanol).	Electrochemical conversion of fuel into electricity using PEMFC or DMFC cells.	High energy density, low noise, zero emissions (for H_2).	System complexity, need for BOP (Balance of Plant), safety of H_2 storage.	Robots for long-term missions — medical, rescue, military CSR.
4.Mains (stationary) power supply.	Constant power supply from the mains via adapter or transformer.	Unlimited operating time, stable voltage.	Limited mobility, need for cable management.	Stationary collaborative manipulators in laboratory and industrial environments.
5. Inductive (contactless) charging.	Energy transfer via electromagnetic induction.	Convenient, automated, no wear of connectors.	Energy losses, limited range.	Robots with periodic charging — hospital and service systems.
6. Solar power or energy recycling.	Photovoltaic panels or energy from vibrations, heat and motion.	Environmentally friendly, additional source for long missions.	Low power, strong dependence on conditions.	Robots for outdoor areas, monitoring or agriculture.

Duration of autonomous operation - requires high energy density (Li-ion, H_2 cell).

- Safety when interacting with people - low voltage
- (≤ 48 V DC), overheating protection, EMC compatibility.
- Maintenance and replacement - modularity of the battery pack, standardized connectors.
- Energy efficiency - minimal losses in converters (DC/DC, DC/AC).
- Mass and distribution of the center of gravity - important for mobile platforms.
- Environmental friendliness and sustainability - recyclable materials, low emissions.

The use of this system of criteria is quite relative and has its importance in determining the power supply system of the collaborative service robot, taking into account the restrictions imposed by the intended use, certain design limitations, and last but not least, its cost and of course the cost of the robot itself. The flowchart links mission requirements, autonomy duration, power dynamics, and mobility constraints to suitable energy solutions, highlighting hybrid fuel cell–battery architectures as a balanced choice for long-duration autonomous operation of mobile collaborative robots.

Example of Power Supply Configuration

Naturally, the selection of the type of power supply for a collaborative robot intended for use in healthcare depends on its purpose. If the robot is intended for intra-hospital transport, one type of power supply is assumed. But if this robot is intended to transport victims of car accidents or to transport them from the battlefield and the robot is capable of high cross-country ability, then obviously its power supply has certain specific requirements. In this case, a power supply is assumed that has a high energy density at a minimum volume and weight, which is sufficiently compact from a structural point of view.

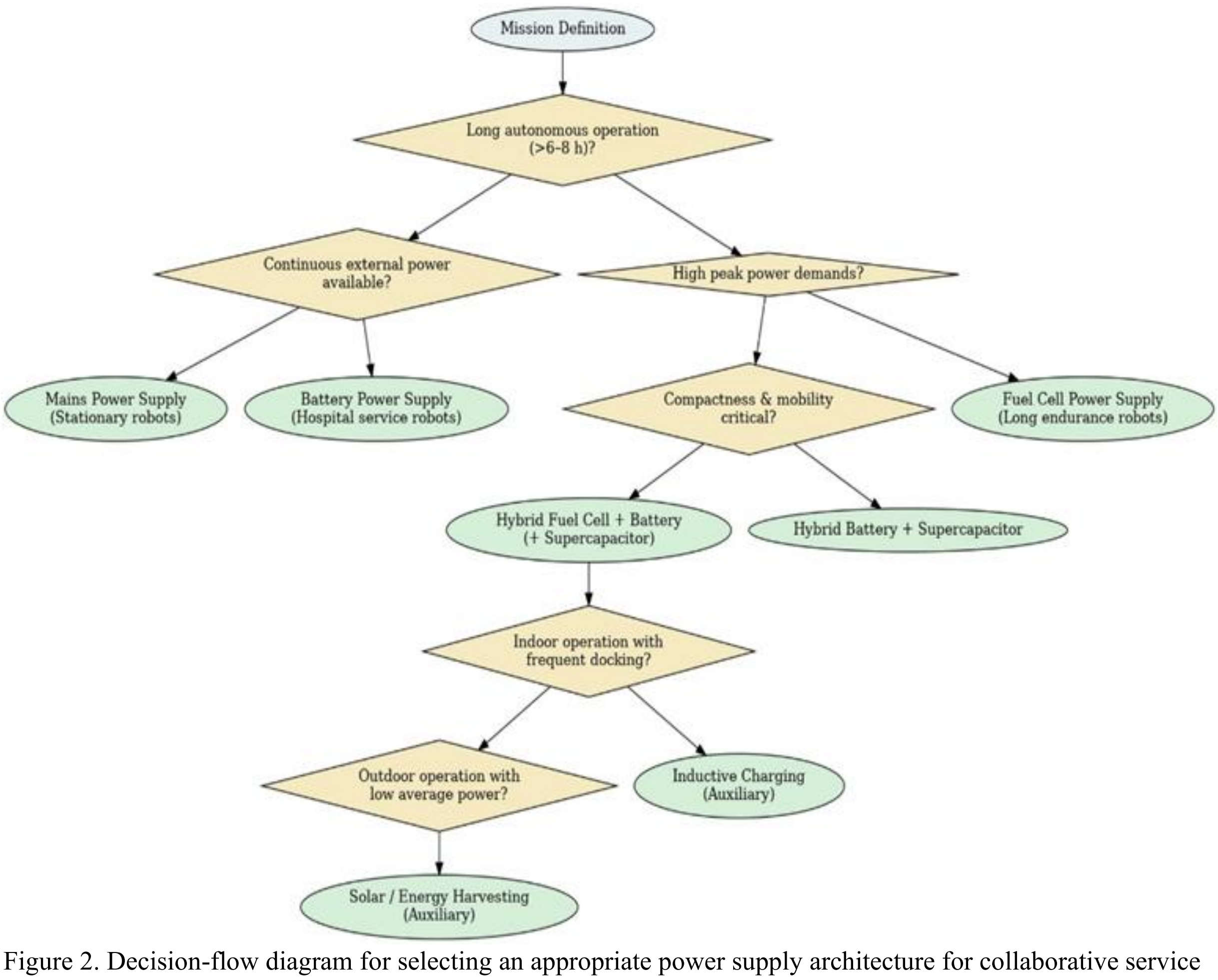

Figure 2. Decision-flow diagram for selecting an appropriate power supply architecture for collaborative service robots

As example of power supply configurations for collaborative robots used in healthcare, the following can be cited, shown in Table 1. It is interesting to analyze the data from Table 2, where the capabilities of a fuel cell combined with a Li-ion buffer so that it represents a hybrid system are immediately noticeable. The possible capacity of activity, which represents more than 12 hours of continuous operation, is remarkable. Of course, this system also has some disadvantages, such as the need to use a hydrogen tank, which is involved in the process of generating electricity. Usually, this is a metal bottle that contains hydrogen and is convenient for quick replacement with a new bottle after the first one is empty.

Table 2. Representative power supply configurations for collaborative service robots

Configuration	Voltage	Capacity	Application
Li-ion 24 V / 20 Ah + BMS	480 Wh	4–6 h autonomy	Small Mobile CSR
$LiFePO_4$ 48 V / 40 Ah	1920 Wh	8–10 h operation	Medium Mobile Platforms
H_2 Fuel Cell 500 W + Li-ion buffer	500 Wh + H_2 tank	> 12 h continuous operation	Hybrid System
AC/DC 230 V → 24 V PSU 500 W	Continuous	Laboratory Environment	Stationary Collaborative Robot

Unfortunately, however, these bottles are significant in size and weight, which makes it difficult to constructively integrate them into the robot. With its huge capacity and ability to work continuously, this power supply system is a suitable solution for integration into a collaborative robot with high cross-country ability, which can operate in rough terrain and carry out transport operations of injured people in the open (Zhou et al., 2024). The remaining systems have their application in collaborative service robots in various cases of use where a high energy flow density is not required and it is relatively easy to recharge them for a new cycle of work (Dunn et al., 2011; Gopi et al., 2024).

Modern Trends

At the modern stage, characterized by the rapid development of Robotics, certain development trends are noticeable (Siegwart et al., 2000). This also applies to robot power supply systems and, in particular, to those systems built into collaborative service robots. With the introduction and development of control systems with elements of artificial intelligence, the management of these systems is becoming increasingly flexible and intelligent. In general, the following development trends in power supply systems can be noted:

- Intelligent energy management systems (Energy Management Systems - EMS) - dynamic distribution of energy between drive, sensors and communication.
- Modular energy architectures - the possibility of adding a secondary source (e.g. H_2 + battery).
- Fast charging stations and automated docking systems - to increase the continuity of work.
- Implementation of safe lithium iron phosphate cells ($LiFePO_4$) in medical collaborative service robots (CSR) due to lower fire hazard and safety in operating modes.
- Application of micro fuel cells and hybrid power units with supercapacitors (Fuel Cell + SC) for robots with a long duty cycle.

A large part of these development trends have already been implanted in real systems powering collaborative service robots. And these are not just laboratory samples, but real systems that perform the most complex service activities by relieving the heavy or monotonous work of people, for example, in healthcare.

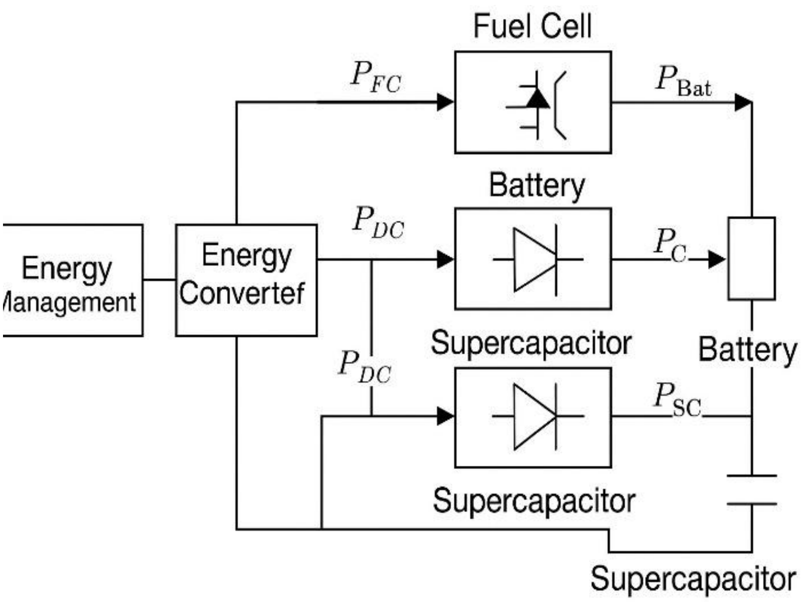

Figure 3. Schematic diagram of a combined power supply with a hybrid block.

The modern development of these systems implies increasingly complex and user-friendly new implementations that will lead to significant help to human society. An exemplary schematic diagram of a combined power supply with a hybrid energy block with supercapacitors and a battery (H2 Fuel Cell + Batt+ SC) for robots with a long duty cycle is shown on Figure 3. Such a configuration involves the use of the advantages of a micro-hydrogen fuel cell with the ability to store part of the energy in a battery. In a situation where significant power is required for a short time, the supercapacitors block is used, through which significant energy can be introduced for a very short time and thus increase the torque of the motors to a value required to overcome the obstacle that has arisen. Such a power supply system is suitable for robots with off-road capabilities in order to perform a task of transporting a seriously injured patient from a random area

Figure 4. Modern collaborative robot

Figure 4 shows a modern collaborative robot with hybrid power supply, a micro hydrogen fuel cell as a hybrid power unit with super capacitors (H2 Fuel Cell + SC) for robots with a long duty cycle. It is a wheeled platform equipped with a rich sensor system, including two types of laser interferometers (LIDAR), with the help of which it orients itself in space and is able to move to any point.

The Fuel Cell

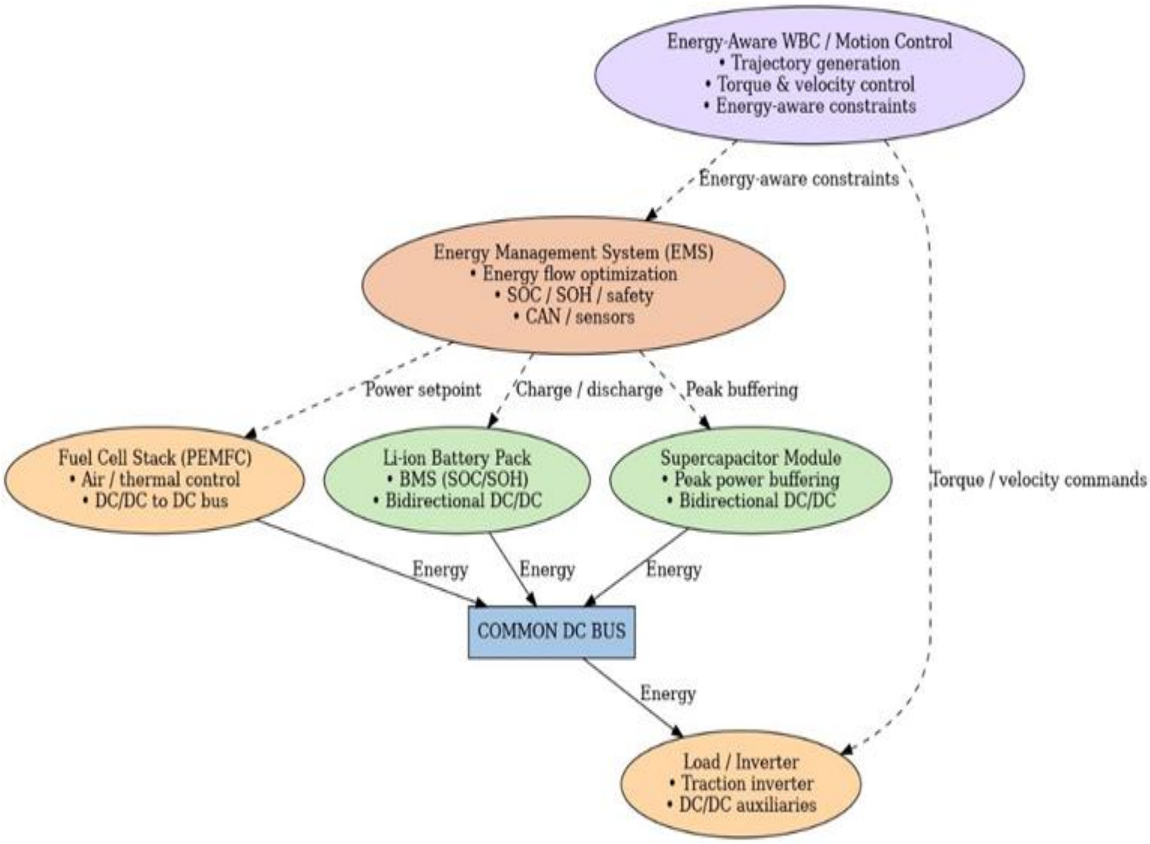

Figure 5. Diagram of the hydrogen fuel supply system of the mobile service collaborative robot.

The idea behind the fuel cell is that, in the presence of a catalyst, the water molecule initially breaks down on the surface of the electrode into two hydrogen atoms and one oxygen atom. By giving up an electron, the hydrogen atoms are oxidized to hydrogen cations. To reach the cathode, the electrons and protons take different paths. The protons pass through a membrane, while the electrons are captured by the cell's external circuit and represent ready-to-use energy. On the cathode side, in the presence of a catalyst, the protons, together with some of the electrons and oxygen, form the waste product (water vapour or pure water) from the operation of the fuel cell.

At the modern stage, characterized by the rapid development of Robotics, certain development trends are noticeable (Zhang, 2026). This also applies to robot power supply systems (Figure 5) and, in particular, to those systems built into collaborative service robots. With the introduction and development of control systems with elements of artificial intelligence, the management of these systems is becoming increasingly flexible and intelligent.

In general, the following development trends in power supply systems can be noted: Intelligent energy management systems - dynamic distribution of energy between drive, sensors and communication and application of micro fuel cells and hybrid power units with super capacitors (Fuel Cell + SC) for robots with a long duty cycle (Radmanesh, 2024).

Mathematical Model of the PEM Fuel Cell

The traction power supply of the Collaborative Robot is based on a low-temperature proton–exchange membrane (PEM) fuel cell stack. The stack voltage is modelled starting from the single-cell voltage, which is expressed as the difference between the reversible Nernst potential and the main loss components:).

$$V_{cell}(i) = E_{Nernst} - V_{act}(i) - V_{ohm}(i) - V_{conct}(i) \quad (1)$$

where i is the cell current density, E_{Nernst} is the open-circuit potential, V_{act} denotes activation losses, V_{ohm} accounts for ohmic losses in the membrane and current collectors and V_{conct} represents concentration (mass-transport) losses.

Final Stage

For the global reaction $H_2 + \frac{1}{2}O_2 \rightarrow H_2O$, the Nernst potential is

$$\mathrm{E}_{Nernst} = \mathrm{E}_0 + \frac{\mathrm{RT}}{2F}\ln\left[\frac{\mathrm{p}_{H2}\sqrt{P_{O2}}}{p^0}\right] \quad (2)$$

where E_0≈1.229V is the standard potential at T_0 =298K and p^0= 1atm, R is the universal gas constant, FFF is Faraday’s constant, and p_H2 and P_O2 are the partial pressures of hydrogen and oxygen at the anode and cathode, respectively. In the operating range considered here, the temperature dependence can be approximated by a linear correction of E_0

Activation, Ohmic and Concentration Losses

Activation overvoltage is described by a Tafel-type relation

$$V_{act}(i) = Aln(i) + B \quad (3)$$

Where: A and B are empirical parameters identified from the low-current region of the polarization curve.

Ohmic losses are modeled as a linear function of current density:

$$\mathrm{V}_{ohm}(\mathrm{i}) = \mathrm{iR}_{ohm} \quad (4)$$

With R_ohm representing the equivalent membrane and contact resistance, which depends on membrane hydration and temperature.

At high current densities, mass-transport limitations are captured by

$$V_{conc}(\mathrm{i}) = -\mathrm{C}ln\left(1 - \frac{\mathrm{i}}{i_{lim}}\right) \tag{5}$$

where i_lim is the limiting current density and C is an empirical concentration-loss coefficient. The parameters A, B, C, Rohmandi _lim are obtained by fitting the model to the manufacturer's polarization curve of the selected stack.

Stack Voltage and Power

The 200 W fuel cell stack consists of N_cell identical cells connected in series, each with active area A cell. For a given stack current I, the corresponding cell current density is:

$$\mathrm{i} = \frac{\mathrm{I}}{A_{cell}} \tag{6}$$

and the stack voltage is:

$$V_{FC}(I) = N_{cell}V_{cell}\left(\frac{I}{A_{cell}}\right) \tag{7}$$

The instantaneous electrical power delivered to the DC bus is then

$$P_{FC}(t) = V_{FC}(I_{(t)})I_{(t)}. \tag{8}$$

For the robot powertrain considered in this work, the stack is dimensioned for a nominal power of 200 W at approximately 48 V, leading to a nominal current of I_{nom}≈4.2 A. The model parameters are tuned such that $V_{FC}I_{(nom)}$≈48 V and the simulated polarization curve closely matches the datasheet.

Dynamic Extension and Simulation Implementation

To capture the transient behavior during rapid load changes, a first-order gas-dynamics model is added for the anode and cathode chambers. The partial pressures p_{H2} and P_{O2} are obtained from molar balance equations.

$$\frac{d_{nk}}{dt} = \dot{n}_{k,in} - \dot{n}_{k,react}, \ \dot{n}_{k,react}, \propto \ I_{(t)} \tag{9}$$

Combined with the ideal gas law. In addition, a double-layer capacitance C_{dl} and charge-transfer resistance R_{ct} form a first-order dynamic model for the activation overvoltage. In the simulation environment, these equations are implemented as a dedicated PEMFC block providing the nonlinear voltage–current characteristic $V_{FC}(I)$ to the hybrid power-supply model of the robot.

Fuel Cell Model Validation and Empirical Analysis

Identified Parameters of the PEM Fuel Cell Model

A summary of the semi-empirical parameters obtained from fitting the fuel-cell model to the reference polarization curve provided by the manufacturer is presented in Table 4. The identified values of the Tafel slope A=0.045V, Tafel intercept B=0.12V and concentration-loss coefficient C=0.015V exhibit typical magnitudes for low-temperature PEM cells operating near ambient conditions. The ohmic resistance R_{ohm}=0.08Ω reflects both membrane resistance and contact losses and is consistent with the expected behavior of compact portable stacks. The estimated limiting current density i_{lim}= 1.8 $\frac{A}{cm^2}$ indicates that the stack can maintain stable operation up to 5 A without entering deep mass-transport limitation. With 68 cells and an active area of 50 cm^2 per cell, the stack achieves a nominal voltage of 48 V at approximately 4.2 A, yielding a rated power of 200 W. The inset box presents the main electrochemical and stack parameters used for system modeling. The inset box presents the main electrochemical and stack parameters used for system modeling.

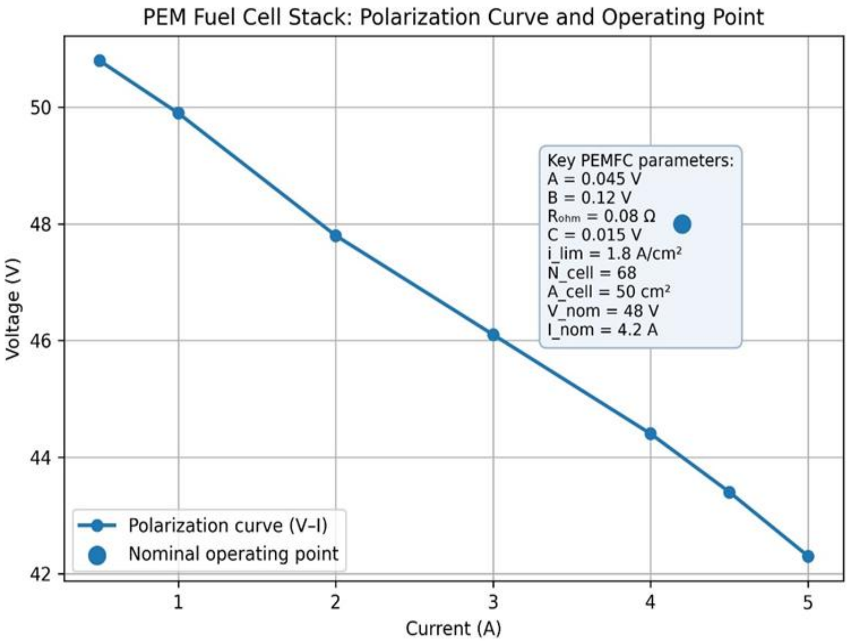

Figure 6. Polarization characteristics and nominal operating point of a PEM fuel cell stack integrated into a hybrid energy system for autonomous mobile collaborative robots.

Model Validation Against Measured Polarization Data

Table 3 presents a direct comparison between measured and modelled stack voltages across a current range of 0.5–5 A. The results demonstrate excellent agreement:

- Absolute error remains below **0.4 V** across the entire operating range.
- Relative error remains below **1%**, even near the high-current region where non-linear effects are more pronounced.

Table 3. Measured vs. modeled polarization data of the 200 W PEMFC stack

Current (A)	Measured Voltage (V)	Modelled Voltage (V)	Absolute Error (V)	Relative Error (%)
0.5	50.8	50.6	0.2	0.39
1.0	49.9	49.7	0.2	0.40
2.0	47.8	47.6	0.2	0.42
3.0	46.1	45.9	0.2	0.43
4.0	44.4	44.1	0.3	0.68
4.5	43.4	43.1	0.3	0.69
5.0	42.3	41.9	0.4	0.95

The smallest errors occur in the mid-current region (2–3 A), where activation and ohmic contributions dominate and are well captured by the semi-empirical formulation. Slightly higher deviations at 4.5–5 A are expected due to concentration effects that are more sensitive to manufacturing tolerances, humidity, and gas supply conditions. Overall, the high fidelity of the model confirms that it is suitable for energy simulation, hybrid-system control design, and performance prediction under variable load conditions.

Electrical Power Characteristics

The electrical output power computed from the measured voltage data is shown on Table 6 As expected for PEMFC technology:

- Power increases almost linearly in the low-current region due to near-constant voltage.

- A distinct **Maximum Power Point (MPP)** appears around **4.5–4.7 A**, where the product V*I reaches approximately **200–210 W**.
- Beyond this point, voltage drops faster than the increase in current, causing power to decline, which is typical of fuel-cell polarization behavior.

This information is particularly important for robot applications because:

- The optimal operating region lies around 80–95% of nominal load.
- Operation far above the MPP leads to higher thermal and membrane stress.
- Operation far below the MPP reduces fuel efficiency.

Table 4. Electrical power of the fuel cell stack as a function of current

Current (A)	Voltage (V)	Electrical Power (W)
0.5	50.8	25.4
1.0	49.9	49.9
2.0	47.8	95.6
3.0	46.1	138.3
4.0	44.4	177.6
4.5	43.4	195.3
5.0	42.3	211.5

Thus, the robot's hybrid powertrain (fuel cell + battery + supercapacitor) should be tuned to maintain average operating current within this efficient band.

Derived Operational Metrics

Table 5 highlights key system-level performance indicators:

- The voltage drop from open-circuit (50.8 V) to nominal load (44.4 V) is consistent with typical PEMFC internal resistance and activation losses.
- The dynamic load range (1–5 A) aligns well with the energy profile of mobile robots during acceleration, cruising, and slope climbing.
- The typical stack electrical efficiency (40–55%) matches manufacturer specifications for compact PEM systems.
- The hydrogen consumption estimate (~0.02 g/s at 4.2 A) provides useful context for autonomy calculations—approximately:
- 1.2 g/min, or
- ~72 g/hour at nominal operating point.

Table 5. Derived performance metrics of the 200 W PEMFC stack

Metric	Value
Maximum power point (MPP)	~4.7 A @ ~43 V
Maximum power	~202–210 W
Voltage drop from no-load to nominal	50.8 V → 44.4 V
Dynamic load range used in robot	1–5 A
Typical system efficiency range	40–55 % (stack-only)
Estimated hydrogen consumption @ 4.2 A	~0.02 g/s (approx.)

For mobile collaborative robots, these values imply practical run-times of several hours depending on tank size and duty cycle.

Simulation Results

This section presents the outcomes of the simulation experiment used to evaluate the performance of the hybrid hydrogen fuel cell–battery power system during a representative 30-minute rescue mission. Three key indicators were analyzed: the robot's electrical power demand and power sharing (Figure 7), the evolution of the battery state of charge (Figure 8), and cumulative hydrogen consumption (Figure 9).

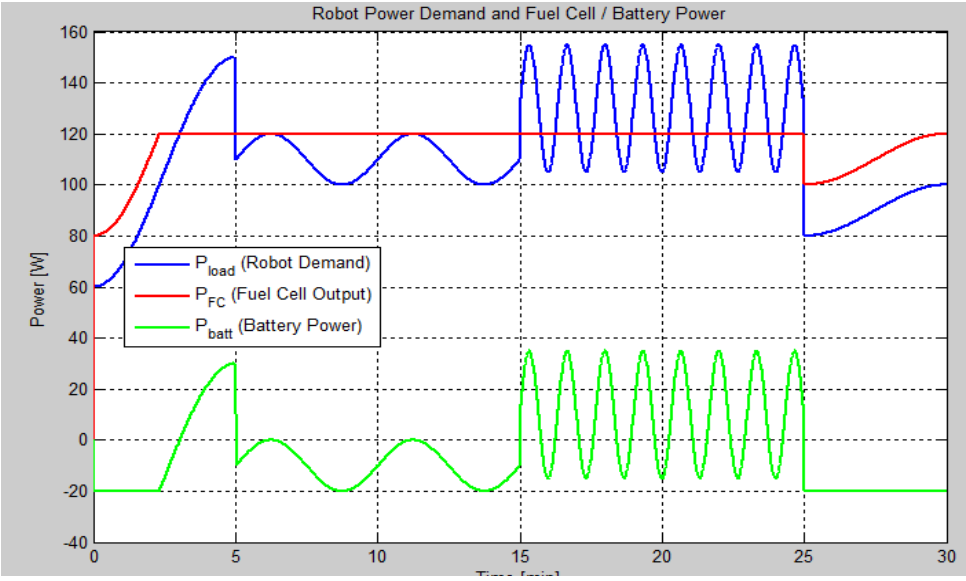

Figure 7. Robot power demand

Power Demand and Power Sharing

Figure 7 shows the interaction between the robot's total electrical power demand (P_{load}), the fuel cell output power (PFC), and the battery power contribution (P_{batt}). The curves capture realistic operating behaviour across four mission phases.

A. Acceleration and initial activity (0–5 min)

P_{load} rises smoothly from ~60 W to ~150 W as the robot accelerates from rest.

- PFC remains near its preferred operating point (~120 W).
- The remaining power (~20–40 W) is supplied by P_{batt} (battery discharge).

This demonstrates the fuel cell's role as a stable energy source and the battery's function as a high-response auxiliary power provider.

B. Steady straight motion (5–15 min)

During straight-line travel, P_{load} stabilizes around 110 ± 10 W.

- PFC closely matches the load.
- P_{batt} oscillates near zero, occasionally negative (charging) when PFC slightly exceeds instantaneous demand.

This reflects efficient hybrid operation with minimal battery cycling.

C. Circular/turning manoeuvres (15–25 min)

Turning and directional adjustments generate higher dynamic loads, oscillating around 130 ± 25 W.

- PFC remains relatively constant (~120 W).
- P_{batt} alternates between positive and negative values, absorbing fast changes and stabilizing the DC bus.

This shows the battery's essential role in compensating for rapid load variations that the fuel cell cannot follow instantaneously.

D. Return and low-speed manoeuvring (25–30 min)

The load reduces to 80–100 W as the robot slows down and stabilizes.

- PFC remains slightly above P_load, resulting in mild battery charging.

Overall, Fig. 5 confirms that the hybrid fuel cell–battery system supports both the baseline continuous demand and transient events typical of a rescue robot.

Battery State of Charge

Figure 8 shows the evolution of the battery state of charge (SOC) during the mission.

- SOC decreases from 80% at the start to approximately 65–70% at the end of 30 minutes.
- This gradual decline indicates:
  - the battery is not overused or overstressed,
  - peak demands are properly buffered,
  - the hybrid system is correctly sized.

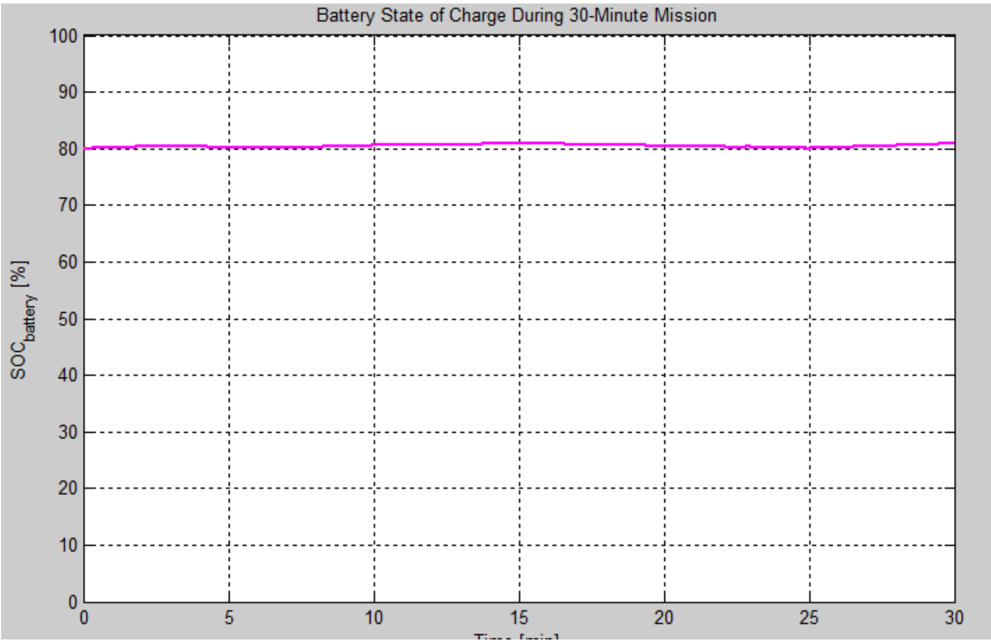

Figure 8. Battery SOC.

Moderate SOC consumption suggests the battery can support significantly longer missions if required.

Hydrogen Consumption

Figure 9 presents the cumulative hydrogen consumption over time, based on the fuel cell's delivered electrical energy and the assumed specific energy of: $1\ \text{kg}\ H_2 = 23\ \text{kWh}$.

- Over the full 30-minute mission, hydrogen usage remains below 6 g, which corresponds to the capacity of the modelled hydrogen cartridge.
- The curve increases smoothly and almost linearly, reflecting the near-constant fuel cell operating power (~120 W).

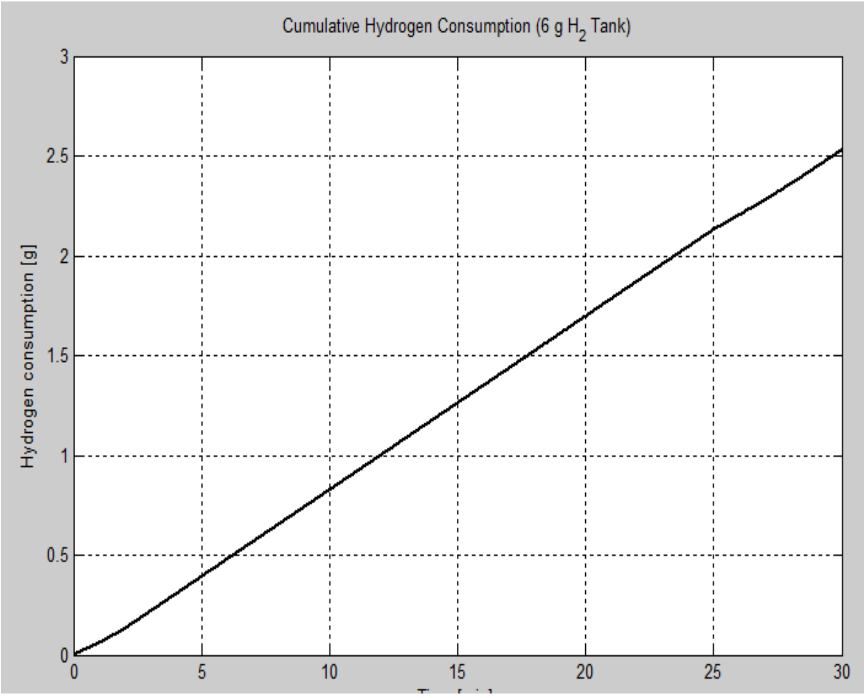

Figure 9. Hydrogen consumption during mission.

This confirms the feasibility of using compact hydrogen cartridges to power service robots in field of medical applications.

Summary of Findings

- The hybrid power system effectively handles dynamic real-world loads (acceleration, steady motion, turning), as shown in Fig. 7.
- Battery SOC remains within a safe, moderate operating band (Fig. 8).
- Hydrogen consumption remains within small-cartridge limits (Fig. 9).

The simulation demonstrates that a hybrid PEM fuel cell–battery system can effectively support the variable load profile of a collaborative rescue robot during a 30-minute mission. The fuel cell provides a stable baseline power level, while the battery supplies fast transient loads during acceleration and turning manoeuvres. The hydrogen consumption remains below 6 g for the entire mission, validating the feasibility of lightweight hydrogen energy modules for field medical robotics. The SOC evolution confirms that the battery experiences moderate cycling, suggesting extended lifetime and high reliability. These results collectively indicate that hydrogen fuel cells, even at small scales, can significantly extend mission autonomy while maintaining stable power delivery under dynamically changing operational conditions.

Link Between Robot Movement, PID Control and Power Profiles

The robot's motion during the simulated mission is governed by a standard PID velocity controller that regulates wheel or track motor speeds in response to the desired velocity profile. The PID loop directly influences both the instantaneous electrical load on the drivetrain and the shape of the P_{load} curve in Fig. 7.

PID Control and Motion Dynamics

The robot uses a closed-loop velocity controller of the form:

$$u(t) = K_P e(t) + K_I \int e(t)dt + K_D \frac{de(t)}{dt} \qquad (1)$$

Where:

- $e(t)$ is the velocity error,
- K_P, K_I, K_D, are the controller gains,
- u(t) is the motor command (torque/current demand).

During the mission:

- Changes in v_rfe (t) (acceleration, turning, deceleration) cause transient velocity errors.
- The PID controller responds with increased motor torque commands.
- Motor torque demand translates directly into increased electrical power demand from the energy subsystem.

This control loop creates the characteristic peaks and oscillations seen in P_{load} in Fig. 7.

How PID Dynamics Shape Fig. 7 (P_{load}, PFC, P_{batt})

A. Acceleration Phase (0–5 min)

At the beginning of motion, velocity error is high.

- The PID proportional term generates large torque requests.
- The derivative term stabilizes the response but also amplifies sharp changes in speed command.

A smooth but pronounced rise in P_{load} (Fig. 7) representing the increased electrical power needed to accelerate the robot.

Battery participation ($P_{batt} > 0$) appears because the fuel cell alone cannot instantaneously supply rapid increases in motor demand.

B. Steady Straight Motion (5–15 min)

Velocity error approaches zero and PID output stabilizes.

- Motor torque requirement becomes nearly constant.
- The controller settles into low-effort regulation.

P_{load} stabilizes around 110 ± 10 W, with minor fluctuations due to noise, micro-corrections, and terrain irregularities.

The fuel cell outputs almost all required power; the battery rests or charges slightly.

C. Circular / Turning Motion (15–25 min)

During turning, left/right wheels or tracks rotate at different speeds.

This causes alternating velocity errors on each side:

- PID controllers on each wheel produce oscillatory torque corrections.
- The robot experiences repeated micro-acceleration and micro-deceleration.

Oscillatory P_{load} around 130 ± 25 W.

These sinusoidal power fluctuations correspond to cyclic correction of velocity error during steering.

Because the fuel cell remains at a stable setpoint (~120 W), the battery absorbs and supplies the difference.

This results in the green P_{batt} curve fluctuating above and below zero.

D. Deceleration / Return Phase (25–30 min)

The desired velocity profile reduces smoothly.

- PID output decreases,
- Motors draw less torque,
- P_{load} decreases to 80–100 W, reflecting reduced kinetic demand.

Some negative P_{batt} values appear as the fuel cell now slightly overpowers the load and recharges the battery.

PID Control Role in Hybrid Power Management

PID-induced torque demands translate into high-frequency power fluctuations at the motor drivers.

Fuel cells cannot respond to high-frequency transients because of:

- slow electrochemical dynamics,
- limited ramp rate,
- efficiency losses under rapid load swings.

Therefore:

- The fuel cell handles *low-frequency, average* power (red curve in Fig. 7).
- The battery handles *high-frequency, transient* power (green curve).

This division of roles is exactly what hybrid FC–battery systems are designed for, and the simulation results visualize this elegantly.

Summary

The dynamic shape of the power demand curve (Fig. 7) is a direct consequence of the PID velocity control loop responsible for regulating wheel/track speeds. Transient velocity errors during acceleration, turning, and manoeuvring generate short-duration torque peaks, which appear in Fig. 1 as oscillations in the P_{load} signal. Because the fuel cell operates optimally at a near-constant power, these PID-induced transients are supplied by the battery (P_{batt}), while the fuel cell maintains the baseline demand (PFC). This behavior confirms the correct functional integration of the hybrid energy system and the motion control subsystem.

Conclusion

The type of power supply for collaborative service robots is determined by the mission, the operating environment and safety requirements. The most flexible solutions are hybrid systems (battery + supercapacitors or battery + fuel cell), which provide an optimal balance between energy density, peak capacity and operational reliability. In future developments, the trend is towards "smart" power modules that self-optimize according to the load and allow collaborative work in a dynamic environment without interruption.Based on the above, the following conclusions can be drawn:

- For mobile collaborative robots: $LiFePO_4$ is preferred due to safety and stability.
- For high-performance platforms or long autonomous missions: the hydrogen fuel cell is an excellent choice.
- For high peak loads and recuperation: supercapacitors are often combined with batteries (hybrid power supply).

This work introduced a comprehensive methodology for the energy-aware design and evaluation of a four-wheeled collaborative robot powered by a hybrid system comprising a 200 W PEM fuel cell, battery storage, and power electronics.

A nonlinear semi-empirical mathematical model of the PEM fuel cell was developed, incorporating activation, ohmic and concentration losses, and validated against measured polarization data. The model demonstrated high fidelity, with a relative voltage error below 1% across the 0.5–5 A operating range, confirming its suitability for energy-flow prediction and hybrid-system optimization. The identification of the stack's maximum-power region (approximately 4.5–4.7 A, 200–210 W) provides a robust reference for controller design and load-sharing strategies.

The methodology is directly applicable to next-generation field-deployable and autonomous service robots operating in energy-constrained environments, where efficiency, reliability, and sustained power delivery are essential. Future research will extend this framework to include adaptive PID tuning, data-driven degradation modeling of the fuel-cell membrane, and hardware-in-the-loop validation using the complete hybrid power system

Scientific Ethics Declaration

* The authors declare that the scientific ethical and legal responsibility of this article published in EPSTEM journal belongs to the authors.

Conflict of Interest

* The authors declare that they have no conflicts of interest.

Funding

* This research received no specific grant from any funding agency in the public, commercial, or not-for-profit sectors.

Acknowledgements or Notes

* This article was presented as an oral presentation at the International Conference on Basic Sciences and Technology (www.icbast.net) held in Konya/Türkiye on April 02-05, 2026.

* The authors acknowledge the financial support of the project with an Administrative Contract under project No. BG-RRP-2.017-0011 "Ecological collaborative robots powered by green hydrogen" under the Recovery and Resilience Mechanism for the implementation of an investment under C2I2 "Increasing the innovation capacity of the Bulgarian Academy of Sciences (BAS) in the field of green and digital technologies" from the Recovery and Resilience Plan.

References

Angelov, G. C. (2025). Green hydrogen generation applied in field mobile robots. *Proceedings of the Bulgarian Academy of Sciences, 78*(9), 1342–1351.

Chinta, S., Bhupathi, H. P., Biradar, V., & Kumar, S. (2025). An analytical research on hydrogen fuel cell technology. *International Journal for Advanced Research in Science & Technology, 15*(2), 168–173.

Delgado Asencio, C., Segura Manzano, F., & Andújar Márquez, J. M. (2025). Hygrobot: Hydrogen-powered mobile robotic platform for rough terrain: Electro-mechanical design, physical implementation, and experimental testing. *Applied Sciences, 15*(9), 5028.

Dunn, B., Kamath, H., & Tarascon, J.-M. (2011). Electrical energy storage for the grid: A battery of choices. *Science, 334*(6058), 928–935.

Ehsani, M., Gao, Y., Longo, S., & Ebrahimi, K. (2018). *Modern electric, hybrid electric, and fuel cell vehicles* (3rd ed.). Boca Raton, FL: CRC Press.

Gopi, C. V. V. M., Ramesh, R., et al. (2024). Review of battery–supercapacitor hybrid energy storage systems. *eTransportation, 22*, 100350.

Hasan, N., Ishraque, M. F., Kamwa, I., Ahmad, K., Alrwaili, A., Alruwaili, M., Amin, N., & Ahmad, N. (2026). Hydrogen and fuel cells as the cornerstones of the universal energy transfer: A comprehensive review. *International Journal of Hydrogen Energy, 209*, 153486.

Kelly, A. (2013). *Mobile robotics: Mathematics, models, and methods*. Cambridge, England: Cambridge University Press.

Lynch, K. M., & Park, F. C. (2017). *Modern robotics: Mechanics, planning, and control*. Cambridge, England: Cambridge University Press.

Miranda, S., Vázquez, C. R., & Navarro-Gutiérrez, M. (2025). Energy consumption analysis and optimization in collaborative robots. *Frontiers in Robotics and AI, 12*, 1671336.

Pa, P. S., & Huang, S. Y. (2016). A design energy system using hydrogen energy and PEMFC for sensing robot. In *Proceedings of the International Symposium on Computer, Consumer and Control (IS3C)* (pp. 112–115).

Radmanesh, H., Farhadi Gharibeh, H., et al. (2024). Energy management of a fuel-cell electric robot based on hydrogen value and battery overcharge control. *World Electric Vehicle Journal, 15*(8), 352.

Siciliano, B., & Khatib, O. (Eds.). (2016). *Springer handbook of robotics* (2nd ed.). Cham, Switzerland: Springer.

Siegwart, R., Nourbakhsh, I. R., & Scaramuzza, D. (2011). *Introduction to autonomous mobile robots* (2nd ed.). Cambridge, MA: MIT Press.

Zhang, Z. (2026). Hydrogen fuel cells. In *Hydrogen energy and fuel cells* (pp. 81–109). Singapore: Springer.

Zhou, J., Qiu, D., Huang, C., Ping, K., & Wen, X. (2024). Energy optimization analysis of robot trajectories and optimization strategies of processing tasks based on time-scaling functions. In *Proceedings of the International Conference on Automation, Robotics and Computer Engineering* (pp. 77–84).

Author(s) Information

Nina Valchkova
Bulgarian Academy of Sciences
Akad. Georgi Bonchev“ str. block 2, Sofia, Bulgaria
ORCID iD: https://orcid.org/0000-0002-8942-7021

Roman Zahariev
Bulgarian Academy of Sciences
Akad. Georgi Bonchev“ str. block 2, Sofia, Bulgaria
ORCID iD: https://orcid.org/0000-0002-9914-3284

Vasil Tsvetkov
Bulgarian Academy of Sciences
Akad. Georgi Bonchev“ str. block 2, Sofia, Bulgaria
ORCID iD: https://orcid.org/0009-0000-9163-1614
*Contact e-mail:*vasil.tsvetkov.ir@gmail.com*

Yasen Paunski
Bulgarian Academy of Sciences
Akad. Georgi Bonchev“ str. block 2, Sofia, Bulgaria
ORCID iD: https://orcid.org/0000-0002-4516-5330

Georgi Angelov
Bulgarian Academy of Sciences
Akad. Georgi Bonchev“ str. block 2, Sofia, Bulgaria
ORCID iD: https://orcid.org/0000-0002-5229-4763

*Corresponding author(s) email

To cite this article:

Valchkova, N., Zahariev, R., Tsvetkov, V., Paunski, Y., & Angelov, G. (2026). Power supply technologies for collaborative service robots: Characteristics and comparative overview. *The Eurasia Proceedings of Science, Technology, Engineering and Mathematics (EPSTEM), 40,* 374-390.